Hierarchically curved gelatin for 3D biomimetic cell culture

Gayatri J. Pahapale[1], Sammy Gao[1], Lewis H. Romer[3-7]*, David H. Gracias[1,2]*

[1]Departments of Chemical and Biomolecular Engineering, [2]Materials Science and Engineering, Johns Hopkins University. 3400 North Charles Street, Baltimore, MD 21218, United States.

[3]Departments of Anesthesiology and Critical Care Medicine, [4]Cell Biology, [5]Biomedical Engineering, [6]Pediatrics, and the [7]Center for Cell Dynamics, The Johns Hopkins School of Medicine, 1800 Orleans Street, Baltimore, MD 21287, United States.

*Co-corresponding authors: dgracias@jhu.edu; lromer@jhmi.edu

TOC Image
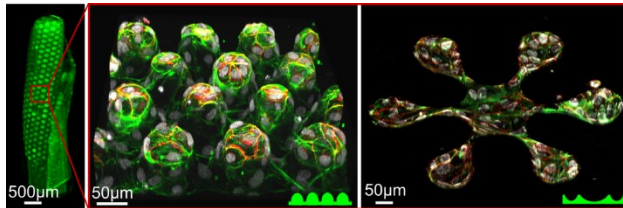
ABSTRACT

The stiffness, micro-curvature, and meso-curvature of cellular microenvironments can significantly alter cell and tissue function. However, it is challenging to produce *in vitro* tissue models that feature tunability in shape, stiffness, and curvature simultaneously in high throughput and cost-effective manner. One of the significant challenges is the fragility of micropatterns in soft and biocompatible hydrogels. Here, we describe an approach that combines reflow photolithography, soft-lithography, and strain engineering to create soft anatomically mimetic gelatin cell culture models. The models can be mechanically tuned to have stiffnesses as low as 400 Pa to as high as 50 kPa featuring hierarchical curvature at two length scales: the cellular length scale of 12 to 120 μm, and the mesoscale of 1 to 4 mm. We characterize the micro-structured gels using optical microscopy and rheometry, highlighting tunability in the hierarchical curvature, modulus, and shape. Also, collagen-based gelatin offers high-level biocompatibility and bypasses the need for additional surface modification to enhance cell adhesion. We anticipate that this approach could advance anatomically accurate *in vitro* 3D cell culture models of relevance to biofabrication, cell biology, and drug screening.

INTRODUCTION

Curving and folding of tissues at multiple levels or orders, defined here as hierarchical, is a typical architectural phenotype found in living systems.[1–3] These geometries provide unique advantages for enhanced surface area, cell viability, and functionality. For example, the dermal-epidermal junction in human skin exhibits an undulating pattern with dermal papillae projecting into the dermis. These projections increase the contact between the layers promoting the exchange of oxygen, nutrients, and waste products.[4] Similarly, hierarchical coiling and curved projections of the small intestine provide a large surface area for nutrient absorption within the limited available volume. These projections include 8-10 mm high *plicae circulares* that extend around the inner circumference of the small intestine, 0.5-1.5 mm tall finger-like villi packed at a density of 10-40 per square millimeter on the *plicae circulares*, and ~ 1μm microvilli that constitute the cellular brush border. Together, these hierarchical projections increase the effective absorptive surface area by a factor of 20.[5–7] Hierarchical curvature is also observed in the human brain in the form of gyri and sulci of the cerebral cortex and folia of the cerebellar cortex. In fact, the gyrification ratio is a commonly used metric to characterize and compare the brains of animals.[8,9] Humans have one of the highest gyrification ratios, which allows the packing of around 100 billion neurons and almost 25 times more glial cells in a highly interconnected fashion.[10] In the lung, gas exchange between the blood and surrounding tissue is facilitated by the highly branched tubular vascular network comprised of vessels with diameters ranging from almost a millimeter (arteries) to 8 μm (capillaries) that interact with the millions of alveoli in the lung.[11] It is necessary to replicate such hierarchically curved tissue microenvironments with

biocompatible hydrogel materials to advance cell studies, create anatomically accurate organs-on-a-chip, and increase the efficacy of a high-throughput drug. Accurate three-dimensional (3D) models are especially important since the geometry of the cell microenvironment has dramatic effects on cell polarization,[12,13] differentiation,[14,15] migration,[16,17] and consequently, drug sensitivity.[18]

Over the past decade, researchers have developed a variety of fabrication approaches to structure cellular materials in curved and folded geometries. These include fiber electrospinning,[19,20] strain engineering,[21,22] selective chemical etching,[17] surface micromilling,[23] lithography and molding,[12,24–29] and 3D printing.[30-32] Strain mismatch in bilayers or pre-stretched membranes has been extensively exploited to mimic the *in vivo* features *in situ*. For example, stress relaxation of biaxially pre-stretched alginate-gelatin methacrylate bilayers has been used to mimic respiratory or gastrointestinal mucosal folding,[21] whereas strain mismatch in metal films[33] or polyethylene glycol diacrylate (PEGDA) bilayers[34,35] has been exploited to make tubes that mimic epithelial ducts. Electrochemical etching of metal sheets has been used to create ultra-smooth sinusoidally wavy surfaces to study the effect substrate topology on cell migration .[17]More recently, 3D printing has been increasingly used to make cell culture platforms as it allows building structural complexity that is present *in vivo*. Some examples include perfusable vascular networks constructed by embedding dissolvable 3D support lattices in a cell-laden hydrogel[30] and models of intestinal villi using live-cell printing with collagen-based bioinks to support both the epithelium layer and a capillary network.[32]

These strategies have significantly advanced the development of *in vitro* cell culture substrates. However, it is still challenging to build model 3D cell culture platforms

with tunable dimensions and geometry. 3D printing is a serial process with limited throughput, is constrained in design, and can be a costly method for patterning features smaller than 50 μm.[36–38] Electrospun mats mimic the fibrous nature of the ECM but exhibit nonuniform cell spreading.[39] Strategies based on techniques like electrochemical etching or laser ablation are complex and not easily accessible, whereas conventional lithographic patterning techniques yield only flat or cuboidal patterns.[40–43] Moreover, these techniques are challenging to implement with soft materials that have a stiffness below 10 kPa.[44] Patterning on soft materials is crucial as matrix stiffness is a major effector in cellular functions like proliferation and differentiation. Early reports of this phenomenon were based upon observations of fibroblasts grown in stressed and relaxed collagen hydrogels. Fibroblasts in stressed gels formed more actin bundles and deposited more matrix in comparison to relaxed gels,[45,46] which was implicated in lung fibrosis.[47] Matrix stiffness has also been demonstrated to have a dramatic effect on stem cell behavior,[48–50] epithelial morphogenesis,[51] and cancer cell migration.[52] Thus, incorporating tunability of matrix stiffness that can achieve physiologic values, together with hierarchical curvature in reproducible and mass-producible cell culture platforms, is crucial for obtaining accurate results in drug discovery and tissue engineering.

Here, we demonstrate a micropatterned gelatin hydrogel platform with tunable stiffness that mimics modulus characteristics of native tissues while also incorporating hierarchical micro to mesoscale curvatures. The micropatterned hydrogel platform resembles features present in epithelial glands, intestinal villi, neo-cortex, and blood vessels. We combine easily scalable technologies, namely lithography and molding, to pattern curved features at the cellular and larger length size scales, creating scaffolds

that may be used as model cell culture platforms. The novel features of our approach are the following: (a) We can micropattern soft as well as stiff substrates with moduli ranging from 400 Pa to 50 kPa; (b) We are able to create curved patterns with a wide range of radii of curvature, from 12 μm to 4 mm; (c) Our approach is compatible with computer aided drawing (CAD) photomask design which allows us to mass produce regular and tunable patterns, with high-fidelity and reproducibility; and (d) our use of gelatin - a naturally cell adhesive derivative of collagen - obviates the need for small molecule or protein adhesive constituents.

MATERIALS AND METHODS

Materials

We purchased gelatin (Type A from porcine skin, Bloom value 90-110 and 300), poly(ethylene glycol) diacrylate (PEGDA, M_n 700), trichloro(1H,1H,2H,2H-perfluorooctyl)silane, and poly(vinyl alcohol) (87-90% hydrolyzed) from Sigma Aldrich (Missouri, USA) and Activa Ti microbial transglutaminase (mTG) preparation from Ajinomoto (Illinois, USA) and used them without any further processing. Positive tone photoresist AZ 9260 (MicroChemicals GmbH) was purchased from Integrated Micromaterials (Texas, USA), and SPR 220 and S1813 were purchased from MicroChem (Texas, USA). Histology section slides for mammalian cerebellum (Catalog# 470182-728), small intestine (Catalog# 470176-962), and arteries (Catalog# 470177-610) were purchased from VWR International and for human skin (Catalog# 470183-070) from Ward's Science.

Substrate fabrication

The strategy for gelatin substrate fabrication is summarized in **Figure 2**. We spin-coated a positive tone photoresist of desired thickness on silicon wafers and patterned it through a photomask using the manufacturer's protocol to create photoresist islands. We then heated the patterned photoresist islands at 150ºC for 20 seconds to induce resist reflow and transform the patterns from a flat to a curved surface.[53]

We silanized the master mold and created negative relief patterns on PDMS (1:10 curing agent to polymer weight ratio cured on the wafer at 80ºC for 1 hour). The resulting PDMS mold had concave features and was used to generate convexities on the gel. A second step of PDMS molding was required to create concave features on the gel. In this case, we silanized the first mold and poured PDMS on top of it to obtain a mold with convex features, which was used to create concavities in the gel. We treated the molds with 1% BSA for one hour to prevent the gel from sticking to the mold, which were then gently washed with DI water, air-dried, and left under UV for at least 2 hours for sterilization.

Next, we prepared the pregel solution (before crosslinking), which consisted of gelatin and mTG. We first dissolved 12.5 wt% gelatin in PBS (Gibco) at 60ºC. In a separate vial, we prepared the mTG solution by dissolving mTG in PBS at a concentration of 10U mTG per gram of gelatin. Both the solution were then sterile filtered through a 0.2 µm filter and mixed to yield the final pregel with a composition of 10 wt% gelatin with 10U mTG per gram of gelatin.[54] We then poured the pregel solution on the PDMS mold and allowed it to crosslink at 37ºC until the desired mechanical properties were achieved. The crosslinked gels were peeled from the mold and heat-treated in PBS at 65ºC for 30

minutes to deactivate the enzyme and dialyze out the reaction byproducts and stored in PBS until use.

We fabricated the gelatin/PEGDA rolls and curved sheets with micro-curved patterns by sequentially crosslinking thin sheets of gelatin and PEGDA, as described by Jamal et.al.[34] with some modifications. We made our chambers for bilayers using the PDMS mold, which had the micro-curved features and a glass slide coated with a sacrificial layer of 10% PVA. We crosslinked the gels using a ruthenium visible light photoinitiator (Catalog #5248, Advanced BioMatrix, CA). The thickness of the gel layer was set by the spacers placed between the PDMS mold and the glass slide during crosslinking. For the pregel solutions, we mixed the contents of the photoinitiator kit with gelatin as recommended by the manufacturer and with PEGDA at one half the recommended concentration. The gels were crosslinked using an LED ring illuminator (~60mW/cm^2, Nikon) held above the chamber at a distance of 2 cm, and then released into PBS. Pregel solutions were filter sterilized using a 0.2 µm filter, and molds and glass slides were sterilized using ethanol or UV light.

Mechanical Characterization

We measured the elastic moduli of the gels by oscillatory shear rheometry using an Anton Paar MCR 302 rheometer. We loaded hydrogel disks (25 mm diameter, 4 mm thickness) hydrated with PBS between a piece of sandpaper and a 25 mm sandblasted plate probe and did all of the measurements at 37ºC. We conducted an amplitude sweep at a constant frequency of 5Hz and 0.5 N normal force.

Cell maintenance and seeding

We cultivated human umbilical vein endothelial cells (HUVEC; ScienCell, Catalog # 8000) in Endothelial cell growth media (PromoCell, Catalog # C22022) at 37°C and 5% CO_2. We seeded the cells on patterned gels at a density of 1×10^5 cells/cm^2. Before seeding the cells, we placed glass rings (Corning, Catalog # 3166-10) around the gels using silicone grease (Dow Corning, Catalog # 1597418) to prevent spreading of cells under the hydrogels and facilitate easy retrieval of the gels **(Figure S1)**.

Cell viability, and immunostaining

We analyzed cell viability on the patterned substrates using a live/dead assay consisting of Calcein AM and ethidium homodimer (Invitrogen™ Catalog# L3224) and performed the test as per the manufacturer's protocol and analyzed the data using epifluorescence imaging (Nikon AZ100).

Before immunostaining, we fixed the cells on the micropatterned gels with a 4% paraformaldehyde solution for 15 mins, which were then permeabilized for 15 minutes with 0.1% Triton X-100 (Sigma Aldrich) in 4% paraformaldehyde and washed with PBS three times. We blocked the fixed samples for one hour with 2% BSA containing 0.01% Triton X-100 (blocking buffer) to prevent non-specific binding of the antibody used. After blocking, we incubated the samples overnight at 4°C with an antibody against VE-cadherin (Rabbit, Cayman Chemicals, Catalog# 160840) prepared in the blocking buffer. We then incubated the samples in a secondary antibody (Cy3 anti-rabbit secondary antibody, Jackson Immuno Research Laboratories, Catalog# 711165152) for one hour. The samples were also stained for F-actin with Alexa Fluor™ 488 Phalloidin (Invitrogen™, Catalog# A12379), and nuclei were labeled with 4',6-Diamidino-2-Phenylindole,

Dihydrochloride (DAPI; Invitrogen™, Catalog # D1306). For imaging, the samples were placed on glass-bottom dishes (MatTek Corporation, Catalog # P35G1.520C) with the patterned surface closer to the objective lens and either mounted in FluorSave (Millipore, Catalog# 345789) or maintained in a humidified chamber. We used a Nikon A1 confocal microscope to image the samples.

RESULTS AND DISCUSSION

Anatomical relevance

Cells in living tissues reside in environments which are hierarchically micro-curved **(Figure 1)** and mechanically diverse. For example, the epidermal-dermal interface of the human skin has undulating folds with radii in the range of 10-50 μm depending on the age, location, and pathology of the tissue **(Figure 1a)**.[55] Similarly, the cells in the intestine
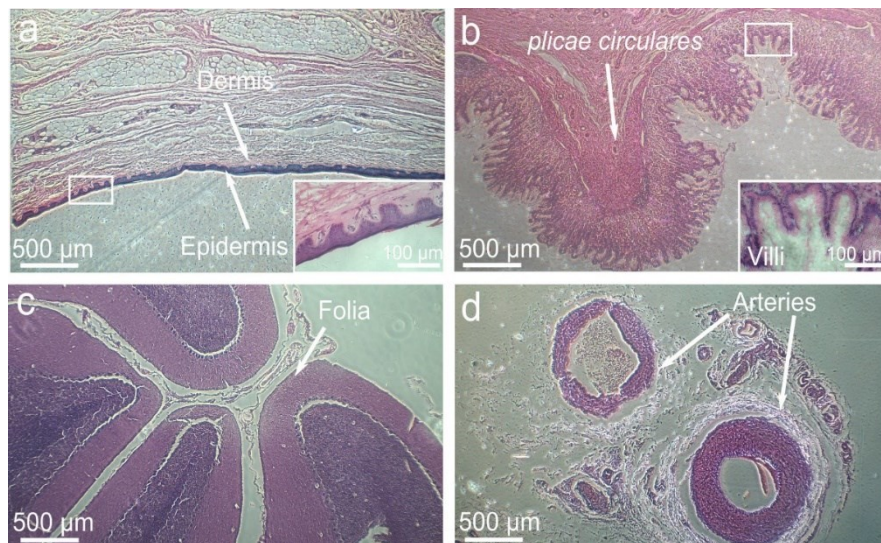

Figure 1. Histology sections of fixed hierarchically curved tissues: (a) Undulating dermal-epidermal interface with an additionally 10x magnified view (inset). **(b)** Longitudinal section of small intestine depicting mesoscale curvature of the *pilcae circulares* and microscale curvature of villi (inset with 10x magnification). **(c)** Cross section of cerebellar folia, and **(d)** transverse sections of mammalian arteries. The histology sections were imaged in our laboratory using a Nikon inverted microscope.

are packed on a curved and folded mucosa as seen in the transverse section of the small intestine **(Figure 1b)** with villus tips having radii in the range of 50-100 µm and elastic moduli in the range of 1 kPa (healthy) to 20 kPa (diseased).[56,57] These heterogeneities in cellular microenvironment, and the broad ranges of variability that are seen with development, disease, and senescence necessitate the innovation of model cell culture platforms that mimic and customize the *in vivo* conditions more accurately.
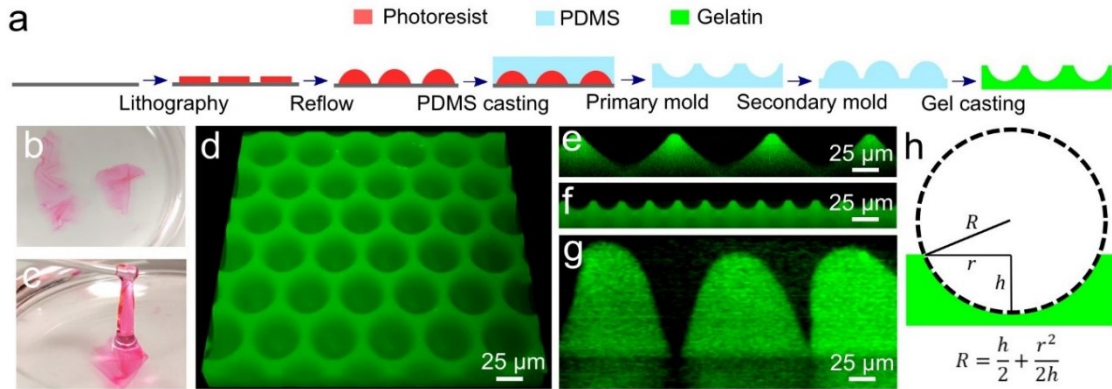

Figure 2. Micro curved gel substrates. (a) The strategy and series of steps used for fabricating the micro-curved features on soft hydrogels are shown. **(b)** 32 µm thick gel sheets were patterned with the micro-curved features. **(c)** Patterned sheets may be transferred between solutions without damage. **(d)** A representative 3D-reconstructed image of the micro-curved gel substrates is shown. Cross-sections of gels demonstrating the tunability of the process correspond to **(e)** lung alveoli, **(f)** the epidermal-dermal interface and **(g)** tips of intestinal villi. **(h)** Determination of the radius of curvature was accomplished by estimating the features as spherical caps, where R is the radius of curvature, h is the height/depth of the curved feature and r is the base radius of the patterned feature.

Our strategy to create micro and mesoscale curved features on soft gels utilizes photolithography, resist reflow, molding, and strain engineering and facilitates tunability for recapitulation of *in vivo* parameters. To make models with a single curvature that mimics the tissue architectures depicted in **Figure 1(a and b)**, we first created the micro

curved features on a silicon wafer using resist reflow lithography **(Figure 2a).** Villi-like features were made by patterning the photoresist using backside exposure to get tapered features and then reflowed to get curved tips. The curved photoresist patterns were then used as masters to make negative molds in PDMS[58] that were then used to pattern sheets or blocks of gel. With this process, we were able to pattern gels with features including radii of curvature in the range of 12-120 µm - reasonable facsimiles of tissues including the tips of intestinal villi, dermal papillae, pulmonary alveoli, and the acini of mammary and sweat glands.

We used gelatin as the primary material for making these micropatterned gels. Gelatin is a protein which thermally crosslinks at room temperature by forming a triple helix. However, it is not stable at temperatures higher than 30ºC and has to be covalently crosslinked for use as a cell culture substrate. Hence, we used microbial transglutaminase (mTG) to covalently crosslink the gel to use it at physiological temperature. mTG crosslinks gelatin by linking the lysine and glutamine residues and hence does not require any chemical modification.[59,60] mTG is also a milder, less toxic crosslinker than glutaraldehyde, EDC/NHS or genipin, and does not plasticize the gel. Importantly, covalently crosslinked gelatin can still undergo coiling at room temperature, and this increases the ease of handling for soft gels.

Gels with micro-curved features may either be made in the form of thin sheets that are several microns thick **(Figure 2 b and c)** or in the form of gel disks with a thickness of one millimeter. **(Figure 3 b and c)**. We allowed thin gels sheets to swell on the mold by immersion in PBS, to release it without causing damage to the patterned features. In contrast, thicker gel disks were peeled directly from their molds. We optically

characterized the prepared gels using confocal microscopy to visualize the micro-curved features. Gels were imaged by dyeing them with fluorescein (Sigma Aldrich, Catalog # F6377) and obtaining z profiles that were reconstructed to view the gels in 3D **(Figure 2d)**. A variety of features of different shapes and scales that mimic *in vivo* geometries may be fabricated with ease, as the technique is dependent only on photomask design and the thickness of the resist **(Table S1)**. The ability to tune the radius of curvature of the features is demonstrated in **Figure 2 (e, f, g),** which depicts cross-sectional views of patterned gels that mimic the curved environments found in lung alveoli, epidermis, and tips of the intestinal villi, respectively. The fidelity and reproducibility of the molding process were confirmed by comparing the designed radii of curvature to the z-profile measurements of the actual gels. For this, we approximated our features as spherical caps and used the acquired z-profiles to estimate the radius of curvature as defined in **Figure 2h**.

We anticipate that these micro-curved patterned gels can be used as models for cell culture studies. Our fabrication strategy is facile and does not employ complex processes like mechanical milling, electrochemical etching, and 3D printing. We can achieve tunable curved shapes even with microscale features in a high throughput manner, which is an advantage over serial processes like 3D printing.

Mechanical characterization

Commercially, gelatin is available in various Bloom values, which indicates the strength of gelatin gel for a given molecular weight. To determine the effect of crosslinking duration and molecular weight on the stiffness, we performed rheological measurements on the mTG-crosslinked gels prepared from gelatin with either of two Bloom values: 90-

110 (Mw$_{av}$~20,000-25,000) or 300 (Mw$_{av}$~50,000-100,000). Based on the rheological measurements we chose lower Bloom value gelatin for soft gels and higher Bloom value gelatin for stiffer gels to tune the gels with physiologically relevant mechanical properties. The mechanical properties were estimated from the linear viscoelastic region (LVER) of the amplitude sweep **(Figure S2)** performed at 0.5 N normal force and a frequency of 5 Hz using a rheometer. We first calculated the shear moduli (G^*), which is defined as $G^* = \sqrt{G'^2 + G''^2}$ where G' and G'' are the storage and loss moduli, respectively, and can be determined from the amplitude sweep **(Figure S2)**. We then estimated the Young's Moduli (E) to compare our gels to tissues and other cell culture materials. Since the gels
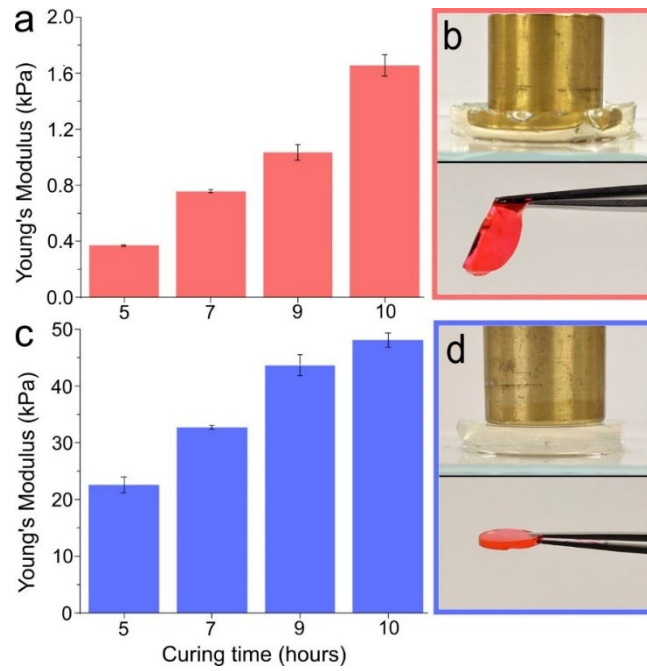

Figure 3. Mechanical properties of the gel are dependent upon Bloom value and curing time. (a) Lower Bloom (90-110) gels or soft gels can be tuned from 400 Pa to 1.8 kPa and **(c)** higher Bloom (300) gels or stiff gels from 20 kPa to 50 kPa. Gel disks with 50 g weight placed on top and 1 mm thick gel disk held with forceps to highlight the difference in mechanical properties of the gels in **(b)** (soft gels) and **(d)** (stiff gels).

are assumed to be isotropic and incompressible under very low strain, the shear modulus can be correlated to Young's modulus using the equation $E = 2G^*(1 + \nu).$ [61,62] The Poisson's ratio (ν) was assumed to be 0.5.[63] **Figure 3 (a and c)** summarizes the effect of Bloom value and crosslinking reaction duration on the mechanical properties of the gels. The Young's moduli of the gels prepared with higher Bloom value gelatin was in the range of 20 - 50 kPa which corresponds to fibrotic or diseased tissue, whereas gels prepared with lower Bloom value gelatin can be tuned in the range of 0.4 - 1.8 kPa which corresponds to soft mucosal tissues and pulmonary interstitial matrices.[64] **Figure 3(b and d)** depict blocks of gel with 50 g weights placed on the surface, as well as gel fragments held with forceps, to give the reader an idea of the gel properties.

Cell culture on micropatterned substrates

Conventionally, mechanically tunable tissue models made from elastomers[65] and gels like polyacrylamide[66] or alginate[67-69] are not cell-adhesive. The surfaces of such models have to be functionalized with adhesion-promoting proteins either by microcontact printing or by chemical conjugation or modification. These surface modification processes often result in uneven distribution of the protein on the gels, and hence to non-uniform cell spreading and surface coverage.

We chose gelatin as our primary substrate material in order to overcome these limitations of surface functionalization. Gelatin is derived from collagen, which is the most abundant component of the extracellular matrix[70]. Gelatin contains the cell adhesion RGD peptide present in its collagen moiety and therefore does not require functionalization. We plated HUVEC on the patterned gels to demonstrate biocompatibility and plating efficiency. **Figure 4** shows the 3D reconstructed images of the gel substrates with

HUVEC, which were fixed after seven days of culture. We estimated the nuclear density per feature and observed less than 15% variance, thus concluding that the cells spread uniformly in concavities and on convexities on both soft and stiff substrates without surface functionalization. The seeded cells were viable for more than one week in culture with minimal cell death occurring due to overgrowth and crowding as depicted by the live/dead assay **(Figure S3)**, demonstrating the biocompatibility of the prepared substrate.
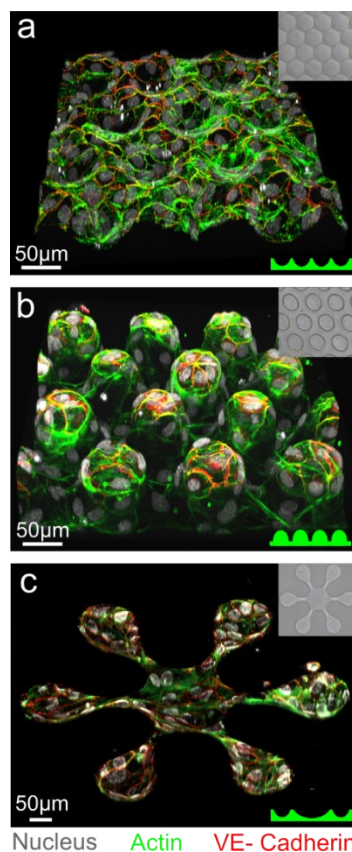

Figure 4. Uniform cell coverage on patterned gelatin hydrogels without surface functionalization. 3D reconstructions of cells seeded on gels patterned with **(a)** concavities with 50 µm radii of curvature, **(b)** tapered pillars with tip radius of curvature of 30 µm, and **(c)** alveolar geometries. Insets depict brightfield images of the top view of the gels (top right in each panel). Cartoons of the cross section of each gel are shown at the bottom right of each panel.

Mesoscale curvature

In vivo tissues are curved and folded at multiple levels. To mimic this characteristic, we fabricated gels curved at a mesoscale. These mesoscale curvatures were created by strain-engineered gelatin, and polyethylene glycol diacrylate (PEGDA) bilayers crosslinked using a visible light ruthenium-based photoinitiator. We sequentially photo-crosslinked thin films of gelatin (1 kPa) and PEGDA (723 kPa) through a CAD designed mask.[34] PEGDA forms an interpenetrating network with gelatin resulting in bilayers that form wavy sheets or tubes when they are released in PBS. For wavy sheets, we patterned squares of PEGDA on a continuous sheet of gelatin to form connected semi-curved regions of PEGDA/ gelatin. Using this process, we can fabricate gels with mesoscale radii of curvature in the range of 1- 4 mm.

Hierarchical curvature

Importantly, as we show, we can combine micro and mesoscale features to create hierarchically curved gelatin substrates **(Figure 5)**. We made these hierarchically curved gelatin substrates by sequentially crosslinking gelatin with PEGDA between the micro curved PDMS mold and a water-soluble sacrificial layer (polyvinylalcohol, PVA) coated glass slide (**Figure S4**). First, we coated the PDMS mold with gelatin mixed with a visible light photoinitiator, covered it with the PVA coated glass slide with spacers in between the slide and the mold, and photocrosslinked the gelatin using visible light. After gelatin crosslinking, we removed the PVA coated glass slide. We observed that the gelatin surface is hydrophobic immediately after crosslinking and does not stick to the PVA and remains on the patterned PDMS mold when the PVA coated glass slide is removed. We then added PEGDA on top of the flat side of the gelatin and placed the PVA coated glass

slide with spacers on top. After photocrosslinking PEGDA, the gelatin/PEGDA bilayer adhered to the PVA coated slide. The bilayer was released from the glass slide by the dissolution of the PVA in PBS to form wavy sheets **(Figure 5a),** or tubes and helices **(Figure 5b, c, and d)**. Cells seeded on to these hierarchically curved bilayers adhered to the microcurved patterns in the outer gelatin layer **(Figure 5e)**.
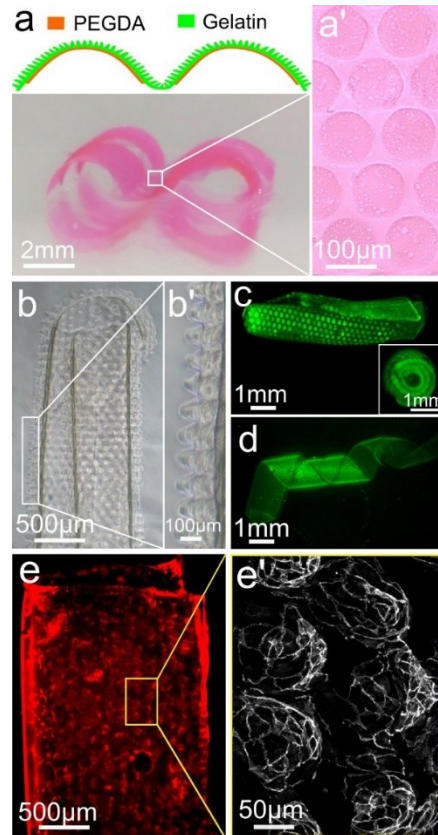

Figure 5. Hierarchically curved gelatin biomimetic substrates. Schematic representation and optical images of **(a)** a curved sheet with **(a')** micro-curved features and **(b), (b')** rolls patterned with micro-curved features to model hierarchically curved tissues. Epifluorescence micrographs of **(c)** a patterned tube depicting the cross-section (inset) and **(d)** self-folded helix with patterns on the gelatin side. The constructs were dyed with fluorescein to visualize the pattern. **(e), (e')** HUVEC seeded on hierarchically patterned rolls labeled for endothelial cell junction (VE-cadherin red in **e** and gray in **e'**).

We note some important features and rationale of our approach. First, the gelatin must be photocrosslinked first, and the PEGDA layer on top of it. We observed that the curing time of gelatin (30 s) is longer than that of PEGDA (15 s), and if the gelatin is photocrosslinked after PEGDA, it leads to over curing of the PEGDA which stiffens this layer and reduces bilayer curvature. Also, we note that the gelatin needs to be crosslinked on the micro-patterned PDMS mold and PEGDA on the flat side of the gelatin layer so that the features are transferred to gelatin. Second, to form a bilayer, an interpenetrating polymer network is required to increase adhesion and prevent delamination on bending. Since gelatin is much more porous as compared to PEGDA, the PEGDA pre-polymer can easily penetrate gelatin and form a robust bilayer on crosslinking. Finally, PEGDA is hydrophilic and sticks to the PVA coating on the glass slide. This adherence facilitates the transfer of the gelatin/PEGDA bilayer to the PVA coated glass slide and subsequent release of the bilayer on the dissolution of the PVA in PBS.

Conclusion

In summary, we have developed a strategy for patterning very soft biocompatible hydrogels with anatomically relevant hierarchically curved geometries. The shapes can be tuned to have cellular length scale radii of curvature of 12-120 μm, and overall radii of curvature from 1 - 4 mm. These parameters mimic *in vivo* morphometrics, including those of intestinal villi, epithelial tissues and their appendages, blood vessels, lung alveoli, and gyri of the brain. The use of standard high-throughput wafer-scale lithography and molding ensures that the process is reproducible, mass-producible, and scalable. The resist reflow transforms the flat lithographic features into curved geometries, while differential swelling generates meso-curvature. We used gelatin as the primary substrate

material as it promotes cell adhesion, and we show that these gelatin-based hydrogels can be mechanically tuned to resemble either soft (0.4 - 1.5 kPa) or stiffer tissues (20-50 kPa). Our gelatin micro-curved substrates offer improved biomimicry with respect to the physical microenvironment of cells with the relative ease of use. We anticipate that this new platform will augment *in vitro* cell culture strategies for studies in which *in vivo* cell and tissue mechanics and microenvironmental geometries need to be closely recapitulated.

ASSOCIATED CONTENT
Supporting Information

Fabrication parameters, amplitude sweep for gels and live/ dead assay of cells.

AUTHOR INFORMATION

Corresponding Author

*E-mail: [1]dgracias@jhu.edu; [2]lromer@jhmi.edu

ORCID

Gayatri J. Pahapale: 0000-0003-2434-0918

Sammy Gao: 0000-0003-2456-089X

David H. Gracias: 0000-0003-2735-4725

Lewis H. Romer: 0000-0002-3780-8500

Present Address

[1] Department of Chemical & Biomolecular Engineering

Johns Hopkins University, 3400 North Charles Street, Baltimore, MD 21218, United States.

[2] Departments of Anesthesiology and Critical Care Medicine

The Johns Hopkins School of Medicine, 1800 Orleans Street, Baltimore, MD 21287, United States.

Author Contributions

G.P., L.H.R. and D.H.G. conceived of the research project. D.H.G. and L.H.R. supervised the experiments. G.P. and S.G. conducted the experiments. G.P. and D.H.G. wrote the manuscript with input from all authors.

NOTES

The authors declare no competing financial interest.

References

(1) Fristrom, D. The Cellular Basis of Epithelial Morphogenesis. A Review. *Tissue Cell* **1988**, *20* (5), 645–690.

(2) Yilmaz, C. O.; Xu, Z. S.; Gracias, D. H. Curved and Folded Micropatterns in 3D Cell Culture and Tissue Engineering. *Methods Cell Biol.* **2014**, *121*, 121–139.

(3) Quiñones, V. A. B.; Zhu, H.; Solovev, A. A.; Mei, Y.; Gracias, D. H. Origami Biosystems: 3D Assembly Methods for Biomedical Applications. *Adv. Biosyst. 2018, p 1800230.*

(4) Ciarletta, P.; Ben Amar, M. Papillary Networks in the Dermal–epidermal Junction of Skin: A Biomechanical Model. *Mech. Res. Commun.* **2012**, *42*, 68–76.

(5) Hilton, W. A. The Morphology and Development of Intestinal Folds and Villi in Vertebrates. *Am. J. Anat.* **1902**, *1* (4), 459–505.

(6) Moog, F. The Lining of the Small Intestine. *Sci. Am.* **1981**, *245* (5), 154–158.

(7) Ensari, A.; Marsh, M. N. Exploring the Villus. *Gastroenterol Hepatol Bed Bench* **2018**, *11* (3), 181–190.

(8) Zilles, K.; Armstrong, E.; Moser, K. H.; Schleicher, A.; Stephan, H. Gyrification in the Cerebral Cortex of Primates. *Brain, Behavior and Evolution* **1989**, pp 143–150.

(9) Welker, W. Why Does Cerebral Cortex Fissure and Fold? In Cerebral Cortex: Comparative Structure and Evolution of Cerebral Cortex, Part II; Jones, E. G., Peters, A., Eds.; Springer US: Boston, MA, **1990**; pp 3–136.

(10) Herculano-Houzel, S. The Human Brain in Numbers: A Linearly Scaled-up Primate Brain. *Front. Hum. Neurosci.* **2009**, *3*, 31.

(11) Ochs, M.; Nyengaard, J. R.; Jung, A.; Knudsen, L.; Voigt, M.; Wahlers, T.; Richter, J.; Gundersen, H. J. G. The Number of Alveoli in the Human Lung. *Am. J. Respir. Crit. Care Med.* **2004**, *169* (1), 120–124.

(12) Sun, B.; Xie, K.; Chen, T.-H.; Lam, R. H. W. Preferred Cell Alignment along Concave Microgrooves. *RSC Adv.* **2017**, *7* (11), 6788–6794.

(13) Yu, S.-M.; Oh, J. M.; Lee, J.; Lee-Kwon, W.; Jung, W.; Amblard, F.; Granick, S.; Cho, Y.-K. Substrate Curvature Affects the Shape, Orientation, and Polarization of Renal Epithelial Cells. *Acta Biomater.* **2018**, *77*, 311–321.

(14) Kilian, K. A.; Bugarija, B.; Lahn, B. T.; Mrksich, M. Geometric Cues for Directing the Differentiation of Mesenchymal Stem Cells. *Proc. Natl. Acad. Sci. U. S. A.* **2010**, *107* (11), 4872–4877.

(15) Zhang, Q.; Lin, S.; Zhang, T.; Tian, T.; Ma, Q.; Xie, X.; Xue, C.; Lin, Y.; Zhu, B.; Cai, X. Curved Microstructures Promote Osteogenesis of Mesenchymal Stem Cells via the RhoA/ROCK Pathway. *Cell Prolif.* **2017**, *50*, e12356.

(16) Werner, M.; Blanquer, S. B. G.; Haimi, S. P.; Korus, G.; Dunlop, J. W. C.; Duda, G. N.; Grijpma, D. W.; Petersen, A. Surface Curvature Differentially Regulates Stem Cell Migration and Differentiation via Altered Attachment Morphology and Nuclear Deformation. *Adv. Sci.* **2017**, *4* (2), 1600347.

(17) Pieuchot, L.; Marteau, J.; Guignandon, A.; Dos Santos, T.; Brigaud, I.; Chauvy, P.-F.; Cloatre, T.; Ponche, A.; Petithory, T.; Rougerie, P.; Vassaux, M.; Milan, JL.; Wakhloo, N.T.; Spangenberg, A.; Bigerelle, M.;Anselme, K. Curvotaxis Directs Cell Migration through Cell-Scale Curvature Landscapes. *Nat. Commun.* **2018**, *9* (1), 3995.

(18) Yu, J.; Carrier, R. L.; March, J. C.; Griffith, L. G. Three Dimensional Human Small Intestine Models for ADME-Tox Studies. *Drug Discov. Today* **2014**, *19* (10), 1587–1594.

(19) Stitzel, J. D.; Pawlowski, K. J.; Wnek, G. E.; Simpson, D. G.; Bowlin, G. L. Arterial Smooth Muscle Cell Proliferation on a Novel Biomimicking, Biodegradable Vascular Graft Scaffold. *J. Biomater. Appl.* **2001**, *16* (1), 22–33.

(20) Christopherson, G. T.; Song, H.; Mao, H.-Q. The Influence of Fiber Diameter of Electrospun Substrates on Neural Stem Cell Differentiation and Proliferation. *Biomaterials* **2009**, *30* (4),

556–564.

(21) Chan, H. F.; Zhao, R.; Parada, G. A.; Meng, H.; Leong, K. W.; Griffith, L. G.; Zhao, X. Folding Artificial Mucosa with Cell-Laden Hydrogels Guided by Mechanics Models. *Proc. Natl. Acad. Sci. U. S. A.* **2018**, *115* (29), 7503–7508.

(22) Tomba, C.; Petithory, T.; Pedron, R.; Airoudj, A.; Di Meglio, I.; Roux, A.; Luchnikov, V. Laser-Assisted Strain Engineering of Thin Elastomer Films to Form Variable Wavy Substrates for Cell Culture. *Small* **2019**, *15* (21), 1900162.

(23) Yu, J. Z.; Korkmaz, E.; Berg, M. I.; LeDuc, P. R.; Ozdoganlar, O. B. Biomimetic Scaffolds with Three-Dimensional Undulated Microtopographies. *Biomaterials* **2017**, *128*, 109–120.

(24) Rettig, J. R.; Folch, A. Large-Scale Single-Cell Trapping and Imaging Using Microwell Arrays. *Anal. Chem.* **2005**, 77 (17), 5628–5634.

(25) Khademhosseini, A.; Eng, G.; Yeh, J.; Fukuda, J.; Blumling, J., 3rd; Langer, R.; Burdick, J. A. Micromolding of Photocrosslinkable Hyaluronic Acid for Cell Encapsulation and Entrapment. *J. Biomed. Mater. Res. A* **2006**, *79* (3), 522–532.

(26) Sung, J. H.; Yu, J.; Luo, D.; Shuler, M. L.; March, J. C. Microscale 3-D Hydrogel Scaffold for Biomimetic Gastrointestinal (GI) Tract Model. *Lab Chip* **2011**, *11* (3), 389–392.

(27) Viswanathan, P., Guvendiren, M., Chua, W., Telerman, S. B., Liakath-Ali, K., Burdick, J. A., & Watt, F. M. Mimicking the topography of the epidermal–dermal interface with elastomer substrates. *Integrative Biology* **2015***, 8(1)*, 21-29.

(28) Serbo, J. V.; Kuo, S.; Lewis, S.; Lehmann, M.; Li, J.; Gracias, D. H.; Romer, L. H. Patterning of Fibroblast and Matrix Anisotropy within 3D Confinement Is Driven by the Cytoskeleton. *Adv. Healthc. Mater.* **2016**, *5* (1), 146–158.

(29) Wang, Y.; Gunasekara, D. B.; Reed, M. I.; DiSalvo, M.; Bultman, S. J.; Sims, C. E.; Magness, S. T.; Allbritton, N. L. A Microengineered Collagen Scaffold for Generating a Polarized Crypt-Villus Architecture of Human Small Intestinal Epithelium. *Biomaterials* **2017**, *128*, 44–55.

(30) Miller, J. S.; Stevens, K. R.; Yang, M. T.; Baker, B. M.; Nguyen, D.H.T.; Cohen, D. M.; Toro, E.; Chen, A. A.; Galie, P. A.; Yu, X.; Chaturvedi, R.; Bhatia, S. N.; Chen, C. S. Rapid Casting of Patterned Vascular Networks for Perfusable Engineered Three-Dimensional Tissues. *Nat. Mater.* **2012**, *11* (9), 768–774.

(31) Song, K. H.; Highley, C. B.; Rouff, A.; Burdick, J. A. Complex 3D-Printed Microchannels within Cell-Degradable Hydrogels. *Adv. Funct. Mater*. **2018**, p 1801331.

(32) Kim, W.; Kim, G. Intestinal Villi Model with Blood Capillaries Fabricated Using Collagen-Based Bioink and Dual-Cell-Printing Process. *ACS Appl. Mater. Interfaces* **2018**, *10* (48), 41185–41196.

(33) Jamal, M.; Bassik, N.; Cho, J.-H.; Randall, C. L.; Gracias, D. H. Directed Growth of Fibroblasts into Three Dimensional Micropatterned Geometries via Self-Assembling Scaffolds. *Biomaterials* **2010**, *31* (7), 1683–1690.

(34) Jamal, M.; Kadam, S. S.; Xiao, R.; Jivan, F.; Onn, T.-M.; Fernandes, R.; Nguyen, T. D.; Gracias, D. H. Bio-Origami Hydrogel Scaffolds Composed of Photocrosslinked PEG Bilayers. *Adv. Healthc. Mater.* **2013**, pp 1142–1150.

(35) Kwag, H. R.; Serbo, J. V.; Korangath, P.; Sukumar, S.; Romer, L. H.; Gracias, D. H. A Self-Folding Hydrogel In Vitro Model for Ductal Carcinoma. *Tissue Eng. Part C Methods* **2016**, *22* (4), 398–407.

(36) Sears, N. A.; Seshadri, D. R.; Dhavalikar, P. S.; Cosgriff-Hernandez, E. A Review of Three-Dimensional Printing in Tissue Engineering. *Tissue Eng. Part B Rev.* **2016**, *22* (4), 298–310.

(37) Albritton, J. L.; Miller, J. S. 3D Bioprinting: Improving in Vitro Models of Metastasis with Heterogeneous Tumor Microenvironments. *Dis. Model. Mech.* **2017**, *10* (1), 3–14.

(38) Mehrotra, S.; Moses, J. C.; Bandyopadhyay, A.; Mandal, B. B. 3D Printing/Bioprinting Based Tailoring of in Vitro Tissue Models: Recent Advances and Challenges. *ACS Appl.*

Bio Mater. **2019**, *2* (4), 1385–1405.

(39) Ma, Z.; Kotaki, M.; Inai, R.; Ramakrishna, S. Potential of Nanofiber Matrix as Tissue-Engineering Scaffolds. *Tissue Eng.* **2005**, *11* (1-2), 101–109.

(40) Chen, C. S.; Mrksich, M.; Huang, S.; Whitesides, G. M.; Ingber, D. E. Geometric Control of Cell Life and Death. *Science* **1997**, *276* (5317), 1425–1428.

(41) Tang, M. D.; Golden, A. P.; Tien, J. Molding of Three-Dimensional Microstructures of Gels. *J. Am. Chem. Soc.* **2003**, *125* (43), 12988–12989.

(42) Rettig, J. R.; Folch, A. Large-Scale Single-Cell Trapping and Imaging Using Microwell Arrays. *Anal. Chem.* **2005**, *77* (17), 5628–5634.

(43) Gommers, L. M. M.; Skrzypek, K.; Bolhuis-Versteeg, L.; Pinckaers, N. E. T.; Vrijhof, R.; van der Wijst, J.; de Baaij, J. H. F.; Stamatialis, D.; Hoenderop, J. G. J. Development Of A Villi-Like Micropatterned Porous Membrane For Intestinal Magnesium And Calcium Uptake Studies. *Acta Biomater.* **2019**,in press.

(44) Bao, M.; Xie, J.; Piruska, A.; Huck, W. T. S. 3D Microniches Reveal the Importance of Cell Size and Shape. *Nat. Commun.* **2017**, *8* (1), 1962.

(45) Halliday, N. L.; Tomasek, J. J. Mechanical Properties of the Extracellular Matrix Influence Fibronectin Fibril Assembly in Vitro. *Exp. Cell Res.* **1995**, *217* (1), 109–117.

(46) Grinnell, F. Fibroblast Biology in Three-Dimensional Collagen Matrices. *Trends Cell Biol.* **2003**, *13* (5), 264–269.

(47) Georges, P. C.; Hui, J.-J.; Gombos, Z.; McCormick, M. E.; Wang, A. Y.; Uemura, M.; Mick, R.; Janmey, P. A.; Furth, E. E.; Wells, R. G. Increased Stiffness of the Rat Liver Precedes Matrix Deposition: Implications for Fibrosis. *Am. J. Physiol. Gastrointest. Liver Physiol.* **2007**, *293* (6), G1147–G1154.

(48) Engler, A. J.; Sen, S.; Sweeney, H. L.; Discher, D. E. Matrix Elasticity Directs Stem Cell Lineage Specification. *Cell* **2006**, *126* (4), 677–689.

(49) Saha, K.; Keung, A. J.; Irwin, E. F.; Li, Y.; Little, L.; Schaffer, D. V.; Healy, K. E. Substrate Modulus Directs Neural Stem Cell Behavior. *Biophys. J.* **2008**, *95* (9), 4426–4438.

(50) Chaudhuri, O.; Gu, L.; Klumpers, D.; Darnell, M.; Bencherif, S. A.; Weaver, J. C.; Huebsch, N.; Lee, H.-P.; Lippens, E.; Duda, G. N.; Mooney, D. J. Hydrogels with Tunable Stress Relaxation Regulate Stem Cell Fate and Activity. *Nat. Mater.* **2016**, *15* (3), 326–334.

(51) Paszek, M. J.; Zahir, N.; Johnson, K. R.; Lakins, J. N.; Rozenberg, G. I.; Gefen, A.; Reinhart-King, C. A.; Margulies, S. S.; Dembo, M.; Boettiger, D.; Hammer, D. A.; Weaver, V. M. Tensional Homeostasis and the Malignant Phenotype. *Cancer Cell* **2005**, *8* (3), 241–254.

(52) Pathak, A.; Kumar, S. Independent Regulation of Tumor Cell Migration by Matrix Stiffness and Confinement. *Proc. Natl. Acad. Sci. U. S. A.* **2012**, *109* (26), 10334–10339.

(53) Daly, D.; Stevens, R. F.; Hutley, M. C.; Davies, N. The Manufacture of Microlenses by Melting Photoresist. *Meas. Sci. and Technol.* **1990**, *1* (8), 759.

(54) Paguirigan, A.; Beebe, D. J. Gelatin Based Microfluidic Devices for Cell Culture. *Lab Chip* **2006**, *6* (3), 407–413.

(55) Jones, P. H.; Harper, S.; Watt, F. M. Stem Cell Patterning and Fate in Human Epidermis. *Cell* **1995**, *80* (1), 83–93.

(56) Johnson, L. A.; Rodansky, E. S.; Sauder, K. L.; Horowitz, J. C.; Mih, J. D.; Tschumperlin, D. J.; Higgins, P. D. Matrix Stiffness Corresponding to Strictured Bowel Induces a Fibrogenic Response in Human Colonic Fibroblasts. *Inflamm. Bowel Dis.* **2013**, *19* (5), 891–903.

(57) Stidham, R. W.; Xu, J.; Johnson, L. A.; Kim, K.; Moons, D. S.; McKenna, B. J.; Rubin, J. M.; Higgins, P. D. R. Ultrasound Elasticity Imaging for Detecting Intestinal Fibrosis and Inflammation in Rats and Humans with Crohn's Disease. *Gastroenterology* **2011**, *141* (3), 819–826.

(58) Xia, Y.; Whitesides, G. M. Soft Lithography. *Angew. Chem. Int. Ed Engl.* **1998**, *37* (5), 550–575.

(59) Aeschlimann, D.; Thomazy, V. Protein Crosslinking in Assembly and Remodelling of Extracellular Matrices: The Role of Transglutaminases. *Connect. Tissue Res.* **2000**, *41* (1), 1–27.

(60) Yung, C. W.; Wu, L. Q.; Tullman, J. A.; Payne, G. F.; Bentley, W. E.; Barbari, T. A. Transglutaminase Crosslinked Gelatin as a Tissue Engineering Scaffold. *J. Biomed. Mater. Res. A* **2007**, *83* (4), 1039–1046.

(61) Landau, L. D.; Lifshitz, E. M.; Sykes, J. B.; Reid, W. H.; Dill, E. H. Theory of Elasticity: Vol. 7 of Course of Theoretical Physics. *Physics Today*. 1960, 44–46.

(62) Vanderhooft, J. L.; Alcoutlabi, M.; Magda, J. J.; Prestwich, G. D. Rheological Properties of Cross-Linked Hyaluronan-Gelatin Hydrogels for Tissue Engineering. *Macromol. Biosci.* **2009**, *9* (1), 20–28.

(63) Rosales, A. M.; Vega, S. L.; DelRio, F. W.; Burdick, J. A.; Anseth, K. S. Hydrogels with Reversible Mechanics to Probe Dynamic Cell Microenvironments. *Angew. Chem. Int. Ed Engl.* **2017**, *56* (40), 12132–12136.

(64) Soucy, P. A., Werbin, J., Heinz, W., Hoh, J. H., & Romer, L. H. Microelastic properties of lung cell-derived extracellular matrix. *Acta Biomater.* **(2011)**, *7*(1), 96-105.

(65) Ruiz, S. A.; Chen, C. S. Microcontact Printing: A Tool to Pattern. *Soft Matter* **2007**, *3* (2), 168–177.

(66) Kandow, C. E.; Georges, P. C.; Janmey, P. A.; Beningo, K. A. Polyacrylamide Hydrogels for Cell Mechanics: Steps toward Optimization and Alternative Uses. *Methods Cell Biol.* **2007**, *83*, 29–46.

(67) Lee, K. Y.; Mooney, D. J. Hydrogels for Tissue Engineering. *Chem. Rev.* **2001**, *101* (7), 1869–1879.

(68) Rowley, J. A.; Mooney, D. J. Alginate Type and RGD Density Control Myoblast Phenotype. *J. Biomed. Mater. Res.* **2002**, *60* (2), 217–223.

(69) Bao, Z.; Xian, C.; Yuan, Q.; Liu, G.; Wu, J. Natural Polymer-Based Hydrogels with Enhanced Mechanical Performances: Preparation, Structure, and Property. *Adv. Healthc. Mater.* **2019**, p 1900670.

(70) Frantz, C.; Stewart, K. M.; Weaver, V. M. The Extracellular Matrix at a Glance. *J. Cell Sci*. **2010**, *123* (24), 4195–4200.

Supporting Information

Hierarchically curved gelatin for 3D biomimetic cell culture

Gayatri J. Pahapale[1], Sammy Gao[1], Lewis H. Romer [3-7,*], David H. Gracias[1,2,*]

[1]Departments of Chemical and Biomolecular Engineering, [2]Materials Science and Engineering, Johns Hopkins University. 3400 North Charles Street, Baltimore, MD 21218, United States.

[3]Departments of Anesthesiology and Critical Care Medicine, [4]Cell Biology, [5]Biomedical Engineering, [6]Pediatrics, and the [7]Center for Cell Dynamics, The Johns Hopkins School of Medicine, 1800 Orleans Street, Baltimore, MD 21287, United States.

*Co-corresponding authors: dgracias@jhu.edu , lromer@jhmi.edu

Table S1: Fabrication parameters and their anatomical relevance

Base radius	Resist height	Curved resist height	Radius of curvature	Anatomical relevance
r (μm)	h$_{resist}$ (μm)	h (μm)	R (μm)	
12.5	8	9 ± 3	12 ± 2	Capillaries, villi tips
25	12	16 ± 3	25 ± 2	Dermis, mammary glands, villi tips
50	25	28 ± 2	54 ± 3	Arterioles
85	35	37 ± 2	117 ± 4	Alveolar glands, arteries, *plicae circulares,* folia
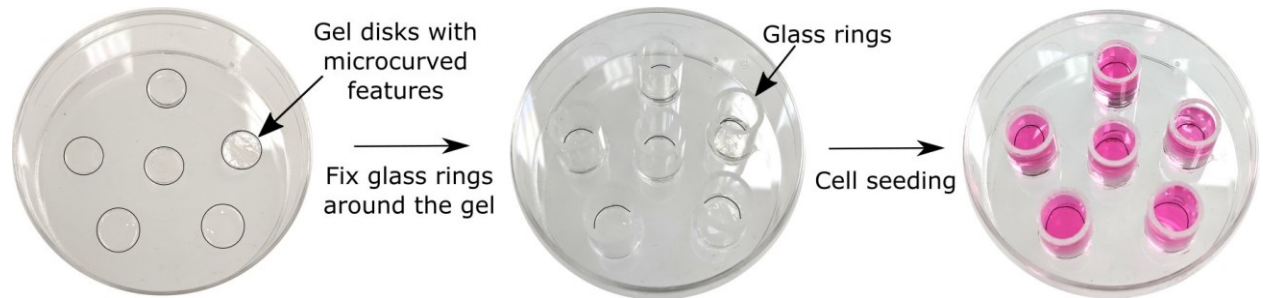
Figure S1: Setup for cell seeding on the hydrogels. Disks of gels patterned with curved features were cut using an 8 mm biopsy punch, and then placed in a plastic dish. Glass rings with inner diameter of 8 mm were snugly attached around these gels and the ends of these rings were coated with silicone grease to form a good seal with the bottom of the dish. Cells were added to the region within each glass ring, to prevent the cells from spreading under the gel and to facilitate retrieval of the gels from the plastic dish for imaging.
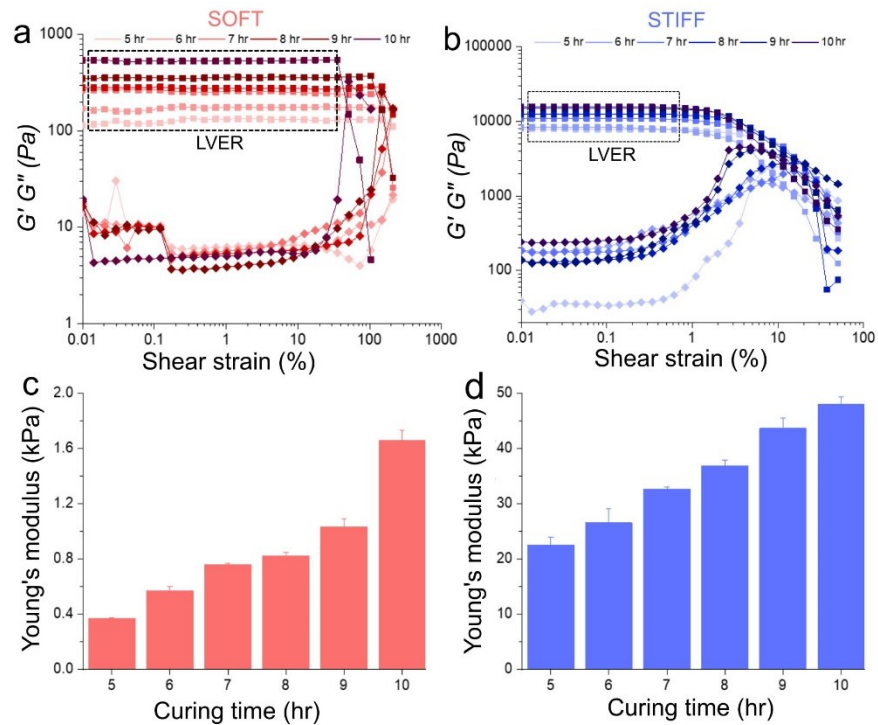
Figure S2. Mechanical and rheological properties of the gel. (a) and (b) Curing time dependent storage moduli (G', squares) and loss moduli (G", diamonds) of the soft and stiff gels respectively and **(c) and (d)** Young's moduli of the soft and stiff gels respectively.
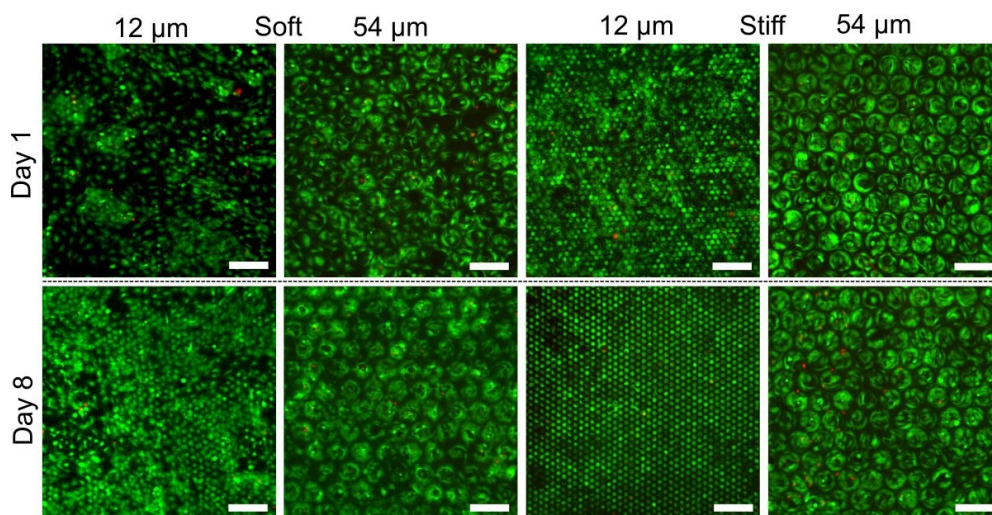

Figure S3. Biocompatibility of the prepared gels. Live dead assay at days one and eight for cells seeded on soft and stiff gels with micropatterned concavities having radii of curvatures 12 µm and 54 µm. Live cells are labeled with Calcein (green) and dead cells are labeled with ethidium homodimer (red). The cells are viable for more than a week with limited cell death that occurs due to cellular overcrowding. Scale bar = 200 µm.
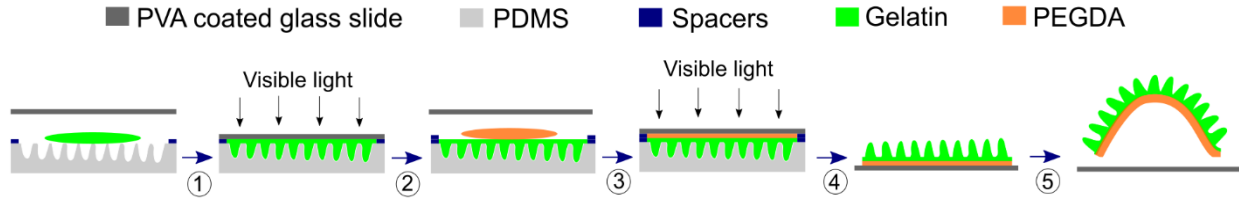
Figure S4: Process flow for the fabrication of hierarchically curved features using gelatin/PEGDA bilayers (images shown in Fig. 5 of the paper). In Step 1, the gelatin mixed with the photoinitiator is added between the PDMS master mold (which is patterned with microurvatures by casting with a resist reflow pattern) and PVA coated glass slide separated by aluminium foil spacers. The gelatin is crosslinked by exposure to visible light. In Step 2, the PVA coated glass slide is removed, and PEGDA prepolymer is added on top of the gelatin. In Step 3, the PVA coated glass slide is placed on the PEGDA and the PEGDA is crosslinked with visible light. In Step 4, the PVA coated glass slide is removed with the PEGDA/gelatin bilayer attached to it. In Step 5, the bilayer spontaneously curves on immersion in PBS due to the dissolution of the PVA sacrificial layer and the swelling mismatch between PEGDA and gelatin.